Dear Copernicus Editors,

This is the map of all the changes applied to the manuscript based on the comments by both anonymous referees in respectively C4720 and C5700. We describe here how we addressed the comments in the text.

C4721: *The authors investigate only the maximum active layer depth, and compare these values over different years in different polygons. No information is given on the timing of these values and on the persistence on the maxima. Would it be possible to investigate the dynamics of the TD for the observation period, analogously to what authors do for soil moisture in Fig. 5? If data are available for such an investigation, it would add value to the paper, highlighting the potential difference in TD dynamics and timing among intact and eroded polygons.*

> We entirely redrawn and rewrote the section on ground thermal regime and active layer depth following the referee's suggestion. Graphs were updated (then fig. 7 and 8 now fig. 6 and 7). Fig. 7 was simplified and therefore can be more intuitively interpreted in our opinion, thus addressing simultaneously the comments by both referees. Details were added to specify and compare between polygons the thaw date initiation, the persistence of the maximum thaw depth and rate of thaw (centimeter/day).

C4721: *In the paper the authors rarely mention the issue of scales. What are the implications of these results at a landscape-scale? The transitions between different equilibria the authors talk about in the section 4.2 can be similar to a large scale transition due to thermo-erosion, such as the one theoretically highlighted by Cresto Aleina et al. (2013)?*

> The issue of scale was discussed in a new subsection in the discussion labeled "The question of scale: time and space".

C4721: *What about time scales? Can the authors discuss the implications of their findings for potential future transitions in more detail? Is there enough evidence to suggest future rapid transitions between two different equilibria? Is the presence of gullies necessary to speed up the thermal erosion process?*

> The issue of scale was discussed in a new subsection in the discussion labeled "The question of scale: time and space".

C4721: *How can your results influence the modeling of such a complex environment? Langner et al. (2013), for example, used a satellite-based approach to model the thermal dynamics in the polygonal tundra. Are there plans to scale up your fine-scale observations to a landscape-scale survey?*

> We discussed this matter in the new discussion

C4721: *Page 11801, line 11: Can you please define what you mean with "active" gully? Does it mean with water flowing through?*

> We reworded the sentence, replacing ‘active’ with ‘a gully experiencing active erosional activity’. We added details regarding the hydrological regime of the water circulating in the gullying network.

C4722: *Page 11802, line 2: please substitute "onsite" with "on site"*

> ‘Onsite’ was replaced by ‘on site’.

C4722: *Page 11802, lines 24-26: What do the authors mean with visually? Could you please specify the accuracy of this evaluation? Please, provide a more detailed description. Maybe a table with the scale description would be of help.*

> Details were added on the acquisition method and the overall visual approach to define the vegetative cover

C4722: *Page 11804, line 12: Please rephrase, the colon does not work well here. I would suggest: "with R..., and graphics..."*

> The colon was replaced and the sentence reworded.

C4722: Page 11805, line 1: is it because of the wind action, or does the snow just fall due to gravity after accumulation?

> The paragraph was reworked to clarify points as suggested by both reviewers. Sentence was reformulated and reference to snow being blown away removed.

C4722: *Page 11806, line 26: What do the authors mean with "active layer depth variability within its grid"?*

> The section mentioning this sentence was rewritten.

C4722: *Page 11807, line 6: the n factor is a ratio in its definition, therefore I would omit this word now, in order not to generate confusion with the n_t factor (line 1, same page).*

> Removed the mention of ‘ratio’.

C4722: *Page 11808: Please, move "anymore" at the end of the sentence.*

> The word ‘anymore’ was moved.

C4722: *Page 11811, line 5: It is rather the interaction, or the synergy of these condition, than the "sum".*

This section was rewritten and this sentence was removed.

C4722: *Page 11811, line 16-17: This sentence is quite vague. Could you please describe this "lesser degree" better, maybe with some quantification?*

This section was rewritten and this sentence was removed in the process.

C4722: *Page 11813, line 6: Please, substitute "Further" with "Furthermore" or similar.*

‘Further’ was replaced by ‘Furthermore’.

C4722: *Figure 2: Probably a typo, but I guess the BYLPD should rather read BYLOTPD, I guess.*

‘BYLPD’ was corrected and changed to ‘BYLOTPD’ in the figure.

C5701: *“Centre” spelling (should be “center”)*.

All occurrences of ‘Centre’ (as in low-centre polygons) were changed to ‘Center’.

C5701: *The authors are not showing data on impacts on greenhouse gases and carbon storage. The last sentence in the abstract is therefore misleading –as written.*

Explicit mention of greenhouse gas was removed and sentence reformulated.

C5701: *To increase readability, I suggest to include references to the supplement in parenthesis, just like you do with regular references.*

Supplements were changed and are now similar to regular references, for instance: “Polygons geometry and instruments specifications are presented in the supplemental material (Supplement 1).”

C5701: *P4, L7: Suggest use a non-value laden term instead of “destroying”. It is also unclear what the authors are referring to in the sentence on P4 L6-9. Please clarify.*

Sentence was removed.

C5701: *Authors are missing some key references […]*

Liljedahl et al. (2012), Walker et al. (2004), and Jorgenson et al. (2006) were added in the introduction section to support the presentation of the context.

C5701: *P5, L7: Leave out "...for this interval".*

"for this interval" was removed.

C5701: *P5, L22: I recommend to be specific about what temperature is referred to, i.e. air or soil? Here, please write soil or ground temperatures, for example.*

We specify which temperatures using 'ground temperatures' instead of only 'temperatures'

C5701: *P5, L22-25: Awkward and unnecessary long sentence. Please fix.*

Sentence was removed

C5702: *How was solid precipitation measured?*

Rain was measured using the 'Hellmann Rain Gauge, compact version' deployed nearby the site. The snow-water equivalent relation was used to account for solid precipitations.

C5702: *P6. L8-10. Please include full sensor name/model and company in parenthesis.*

We inserted a table (previously Supplement 1), into the text, specifying the state of the polygons, their size, the sensors used for each sites and what was their model and company name.

C5702: *P6. L10-11. Awkward sentence. Suggest replace "obtained" with "estimated" or "calculated"*

We replaced "obtained" with "calculated" and overall reformulated the sentence.

C5702: *P6. L12-13. Please be clear. What "data" are you referring to? Each sentence are to be able to stand on its own to be a strong and easily understandable sentence and therefore, manuscript.*

We made precisions about which data : "Calibration of the moisture data recorded by the TDR probes was necessary […]". Further we will make sure each sentence in the manuscript stand on its own.

C5702: *P6, L10-18: You are referring to the supplement for details, but then you are providing details. I suggest providing a basic approach in the manuscript, while leaving the details to the supplement.*

> In the supplement, we initially presented a summary of the ground moisture data, while in the text we detailed how and why the calibration was performed on the raw data. While rewriting the results on moisture we changed how we presented the data. Data was presented in Figs. 5 and 6 and in the text: we therefore removed the Supplement detailing raw moisture data.

C5702: *P6. L19-22: What does "snow conditions" mean? Please be clear as it can mean a lot of things. I want to know what was measured.*

> We reworded 'Snow conditions' to the more specific expression 'Maximum snow depth'.

C5702: *P6, L24: If you do not intend to present the larger study, then omit that reference as it would be irrelevant.*

> We put a reference about the larger study to add context.

C5702: P7, *L3: Lacking details. Please clarify what you mean with "to ascertain that sites were similar to 2010".*

> The sentence was removed.

C5702: *P8, L14-17: Please provide more details here (and omit them in the supplement) on how the ground elevation survey was designed and performed. There is a challenge to survey these landscapes due to the "fluffy" organic mats, so what is the estimated error?*

> We expanded in the text how the survey was accomplished (…92 to 210 spatially referenced points were recorded for each polygons…), presented accuracy and error calculation, and how the 3D surface was built. We removed in this version of the manuscript the related supplement (Supplement 3 in the first version).

C5702: *P9. L1: Was the snow blown away inside the gully? The sentence is confusing to read.*

> Sentence was reformulated and reference to snow being blown away removed.

C5702: *P9. L3-4: This is the results section, not the background section so please move references to the background/site description.*

Reference was removed and sentence reformulated.

C5702: *Figure 2-4. Can figure 2 through 4 be combined into one figure?*

Figure 2 have a different role from Figure 3 and 4 with a scale encompassing the whole study area and indicating where each stations and subsites are; in addition Figure 2 is often referred to in the manuscript. We changed Figure 3 and 4 by standardizing both (scale, and topographical background) and compacted both in two fitting sub-figures (3a and 3b).

C5703: *Can the polygon names, which are currently numbers, be replaced with a name that describes what makes each polygon/study site unique?*

Polygon names were changed: 331 = EP-A, 333 = EP-B, 563 = EP-C, 573 = IP-A. Every references to the polygon names, either in the text, the tables or the figures, were changed to the new denomination.

C5703: *P9. L21-26: This description is rather unclear and vague. What time periods do you refer to etc?*

We reworded the sentence and now point to the proper time period. Clarifications were also made.

C5703: *P9-10: I find the presentation of the soil moisture data and the different polygons thin and confusing, Figure 5 is quite descriptive and I think the authors can strengthen their written description of the results from Figure 5 and use Figure 6 as a supporting display. To me, it looks like the overall seasonal variability is too large between all the polygons to clearly say that the eroded versus intact polygons are significantly different. I hope this is discussed in the discussion? (I suspect this may have to do with the degree/extent/details of erosion at respective polygon and in general, the large variability in these landscapes).*

The presentation of the moisture data (Ground moisture and cover subsection) was extensively rewritten to strengthen the results, as suggested.

C5703: *Figure 6. Please expand the figure caption so it clearly explain what the information in the figure represent. For example, the x-axis is not explained effectively.*

We specify in the figure caption the meaning of the relation between variables presented.

C5703: *Sometimes the authors use “eroded” and sometime they use “breached”. Please stick to one term/naming style.*

We reviewed the text and changed occurrences of “breached” to “eroded” when one could be replaced with the other, as suggested.

C5703: *If the polygons were flooded and therefore, the near-surface soil saturated (and thawed), then the authors may consider to present their soil moisture data as percent saturation, which is a relative metric instead of an absolute metric (see Hinzman et al 1991). I think it can help simplify the rather comprehensive soil moisture dataset and aid site-to-site comparisons.*

Figures presenting moisture data (initially Figure 5 and 6, now renamed Figure 4 and 5) were changed to reflect the percent-saturation of the near surface as suggested, thus replacing the volumetric water content. In the text, values were changed to express the percent-saturation instead of the volumetric water content.

Supplement 2 was presenting basic statistics on volumetric water contents for each sensors (such as minimums, maximums, standard deviation, etc…). Since the presented data is now a relative metric (percent-saturation) replacing an absolute metric (VWC), we assumed that it would not be mathematically relevant to display an updated supplement with detailed basic statistics and thus removed the related supplement.

C5703: *Figure 7. I suggest giving the “intact” polygon a separate symbol – assuming that the story of the manuscript is how the intact versus the eroded polygons differ (??)*

The intact polygon symbol was changed – now a square instead of a circle. Figure 7 is now labeled Figure 6.

C5704: *Figure 8. This figure is not readable. […] Instead, perhaps focus on presenting only temperature from one depth and plot all sites in the same figure (?) [..]*

Comments by anonymous referee #1 suggested that we present and discussed more thoroughly on active layer dynamics and the thermal regime. Therefore to addresses both comment, we rebuilt the figure and simplified it so it focuses especially on the thaw depth (now Fig. 7). We reduced the temperature gradient from one degree per level to 4, 8, 16 degree per level.

Considering how the sensors were deployed in the field by various staff, projects and timing, not all sites were instrumented the exact same way: EP-C had a sensor at 25 cm, other sites at 20 cm, no surface sensor were installed for BYLOTPD, thus complicating the representation of the temperature comparison at similar depths. The approach of interpolation of the temperatures for each sites enabled a simple way to graphically represent emplacements instrumented using slight differences between each other.

C5704: P13-15: *The discussion section is poorly supported by the presentation in the result section, which results in a weak discussion section. I think you need to rebuild the result section and lift out your story more effectively, then you'll have an easier task to write a discussion section that is supported by your data. Also, a large section of the discussion (P14, L1-14) reads like a literature review and in general, a repetition of what was already said in the introduction.*

> Following the reorganisation of a major section of the "Results", the discussion was rewritten entirely. When relevant, some elements were reused from the original text. Repetitions were avoided.

C5704: P 15-17: *The section about "Variability: Implication" seems like a side story. I suggest to remove or alternatively, place into the supplemental (if the authors can more effectively link it to their dataset/story).*

> Section was entirely removed. When relevant, some elements were re-used. Partial elements from p. 11812 L15-26 from the original document were inserted in the p. 20 of the new document.

C5704: P 17. L20-22. *I disagree with the first statement (": : : intact low center polygons: : :were homogenous in the center and between each other"). I only saw data from one intact low center polygon presented! So of course you have a 100% homogeneous match! I agree with your interpretation of data in the following*

> We changed how we present our conclusions to not be biased such as suggested by the referee.

Supplements were restructured. Supplement 4 in the original version of the manuscript presenting the plant cover for each sites, is now the sole supplement (Supplement 1), other were integrated in the text.

Some references were added and removed, as the text was rewritten.

The title was changed.

Results, discussion and conclusions were extensively rewritten.

Finally, we rechecked and worked on the quality of the English in the overall text.

Cordially,

Etienne Godin.

References

Jorgenson, M. T., Y. L. Shur, and E. R. Pullman. 2006. Abrupt increase in permafrost degradation in Arctic Alaska. Geophysical Research Letters 33:L02503.

Lara, M. J., A. D. McGuire, E. S. Euskirchen, C. E. Tweedie, K. M. Hinkel, A. N. Skurikhin, V. E. Romanovsky, G. Grosse, W. R. Bolton, and H. Genet. 2015. Polygonal tundra geomorphological change in response to warming alters future CO2 and CH4 flux on the Barrow Peninsula. Global Change Biology 21:1634–1651.

Liljedahl, A. K., L. Hinzman, and S. J. 2012. Ice-Wedge polygon type controls low-gradient watershed-scale hydrology. Pages 231–236 *in* K. M. Hinkel, editor. Proceedings of the Tenth International Conference on Permafrost. . The Northern Publisher Salekhard, Salerkhard, Yamal-Nenets Autonomous District, Russia.

Walker, D. A., H. E. Epstein, W. A. Gould, A. M. Kelley, A. N. Kade, J. A. Knudson, W. B. Krantz, G. Michaelson, R. A. Peterson, C.-L. Ping, M. K. Raynolds, V. E. Romanovsky, and Y. Shur. 2004. Frost-boil ecosystems: complex interactions between landforms, soils, vegetation and climate. Permafrost and Periglacial Processes 15:171–188.

Summary
2016-01-04 5:18:38 PM

Differences exist between documents.

New Document:	**Old Document:**
bg-2015-317-manuscript-v2	bgd-12-11797-2015
39 pages (5.57 MB)	35 pages (2.40 MB)
2016-01-04 5:18:15 PM	2016-01-04 5:18:15 PM
Used to display results.	

Get started: first change is on page 1.

No pages were deleted

How to read this report

Highlight indicates a change.
~~**Deleted**~~ indicates deleted content.
indicates pages were changed.
indicates pages were moved.

Manuscript prepared for Biogeosciences Discuss.
with version 2015/04/24 7.83 Copernicus papers of the LATEX class copernicus.cls.
Date: 26 December 2015

Nonlinear thermal and moisture response of ice-wedge polygons to permafrost disturbance increases heterogeneity of high Arctic wetland

E. Godin[1,3], D. Fortier[1,3], and E. Lévesque[2,3]

[1]Université de Montréal, Montréal, Québec, Canada
[2]Université du Québec à Trois-Rivières, Trois-Rivières, Québec, Canada
[3]Center for Northern Studies, Laval University, Québec, Québec, Canada

Correspondence to: E. Godin (etienne.godin@gmail.com)

Abstract

Low-center polygonal terrains with gentle sloping surfaces and lowlands in the high Arctic has a potential to retain water in the lower central portion of ice-wedge polygons and as such are considered high latitude wetlands. Such wetlands in the continuous permafrost regions have an important ecological role in an otherwise generally arid region. In the valley of the glacier C-79 on Bylot Island (Nunavut, Canada), thermal erosion gullies were rapidly eroding the permafrost along ice wedges affecting the integrity of the polygons by breaching and collapsing the surrounding rims. Intact polygons were characterized by a relative homogeneity in terms of topography, snow cover, maximum active layer thaw depth, ground moisture content, vegetation cover where eroded polygons responded non-linearly to perturbations which resulted in differing conditions in the latter elements. The heterogeneous nature of disturbed terrains impacted active layer thickness, ground ice aggradation in the upper portion of permafrost, soil moisture, vegetation dynamics and carbon storage.

1 Introduction

Ice-wedge polygons as non-sorted patterned ground terrain type (Ballantyne, 2007) are widespread in the continuous permafrost zone characterizing the high Arctic (Black, 1976; Mackay and MacKay, 1974). High latitude valleys (Dostovalov and Popov, 1963) and more generally arctic lowlands are prone to the formation of low-center polygon fields, which often typify a poor drainage and predominantly wet terrain (French, 2007; Zoltai and Tarnocai, 1975). Low center polygons in arctic wetlands often develop ponds in their centers (Black, 1976) and are considered to have an important ecological role enabling suitable habitats for various macro species, either plants or animals (Gauthier et al., 1996, 2005, 2011, 2013; Jia et al., 2003; Massé et al., 2001; Myers-Smith et al., 2011; Woo and Young, 2012; Walker et al., 2004). Ponds and lakes commonly form in such polygonal wetlands that can act as carbon sinks or GHG source (Tranvik et al., 2009; Bouchard et al., 2015) therefore playing an important role in the global carbon cycle.

The main input of water in the polygons is snowmelt while evapo-transpiration contributes to water loss. The integrity of the polygon rims, the depth of active layer and the lateral flow within the active layer further contribute to the dynamics of the storage (Helbig et al., 2013; Liljedahl et al., 2012). Distinct terrain units in a permafrost landscape (ex: polygons, ponds, hummocky terrain) can develop and co-exist over very short distances (a few meters between each terrain units) with perceptible differences among physical characteristics, such as the active layer depth, the ground temperature and the hydrological conditions (Boudreau and Rouse, 1995). A survey at the polygon scale demonstrated significant differences in the water balance, active layer depth and plant distribution among single polygons located in similar lowland mires but distant from each other by a few kilometers (Minke et al., 2009) further stressing intra-site variability for almost identical terrain units. Another study demonstrated the variability in active layer depths in a non-disturbed and uniform 5 km^2 grid with high and low center polygons (Gangodagamage et al., 2014).

Generally, permafrost disturbance and degradation exert a range of impacts on the affected area, such as, but not limited, to ecosystem shifts and consequent changes in topography and mass transfer (Jorgenson and Osterkamp, 2005; Godin et al., 2014). When disturbance occurs in wet polygons, water could be transferred from centers to collapsed troughs when polygons evolve from low-center to high-center. The presence of dead tussock in the high-center polygon provide evidences of previous, moister conditions (Jorgenson et al., 2006). Furthermore, subsidence in the scale of a few centimeters in a very low gradient landscape can exert a major impact on the hydrology of a watershed (Liljedahl et al., 2012). Disturbances in polygon fields such as by thermo-erosion gullying of ice wedges can occur very rapidly, with severe and immediate impacts on the terrain hydrology and ecological integrity (Fortier et al., 2007). On Bylot Island, one single gully eroded hundreds of polygon ridges over a period of fourteen years and clear changes were observed in polygon moisture and vegetation conditions (Godin et al., 2014; Perreault, 2012; Perreault et al., 2015). Changes in cover and surface aspects are obvious near the gullied area and vary between eroded and intact polygons. Physical differences between a closed-rim polygon (intact) and an open one (due to gullying) located only a few meters apart can induce very different plant communities in their respective center in response to changing moisture and active layer conditions (Perreault et al., 2015). Vegetation changes in wetlands have direct implications on the food web: for instance in the Baffin area (and on Bylot Island), large avian herbivore populations rely on graminoids for support and the most adequate land unit (i.e. wetland) for this type of vegetation is restricted (Gauthier et al., 1996). Few detailed studies were conducted at the polygon scale with a specific focus on their thermal or moisture evolution through time while considering their micro-topography (Helbig et al., 2013; Minke et al., 2009).

This paper discusses the implications of the polygon ridges erosion by gullying and how this changed the microtopography, near-surface moisture conditions, active layer dynamics and vegetation distribution. This will be examined by comparing the aforementioned factors between undisturbed and eroded polygons.

2 Methods

2.1 Study site

The study site is located in the valley of the glacier C-79 (locally known as Qalikturvik valley) in the western part of Bylot Island in the eastern Canadian Arctic archipelago (73°09′ N 79°57′ W) (Fig. 1a). The 4 km wide per 17 km long glacierized valley (Fig. 1b) is drained via a proglacial braided river connected to the Navy Board Inlet (Inland Water Branch, 1969). The pro-glacial river is bordered by a syngenetic ice-wedge polygon terrace composed of layers of loess and poorly decomposed peat (Fig. 2) (Fortier and Allard, 2004). Polygons in the valley have either high center or low center and thousands of lakes and ponds are scattered over the terrace. Groups of high center polygons are often surrounded by linear ponds that formed over ice wedges following collapse of polygon ridges (Bouchard et al., 2015). Several thermo-erosion gullies developed through the valley and increased the hydrological connectivity between the valley walls and the river (Godin and Fortier, 2012a; Godin et al., 2014).

Climate normals (1981–2010) were recorded at the Pond Inlet airport meteorological station at 62 m a.s.l. (Environment Canada, 2014) on Baffin Island, 85 km south-east from the study site. Daily average air temperature was −14.6 °C and precipitation 189 mm (91 mm of rain). A cross-correlation analysis revealed close correspondence between observations at the Pond Inlet airport and those in the Qalikturvik valley (Fortier and Allard, 2005; Gauthier et al., 2013). Daily average air temperature for the 1994–2013 interval at the study site was −14.5 °C (CEN, 2014).

Four polygons located nearby a gully (labeled R08) experiencing active erosional activity (Godin et al., 2014) were instrumented (Fig. 2). Discharge in the gully reached 1 $m^3 s^{-1}$ due to the freshet and diminished rapidly to a total cessation during July except when substantial precipitation occurred (Godin et al., 2014).

Three of those polygons were partially eroded during the development of the gully, and the fourth remained intact. These three polygons were initially eroded in 1999 and early 2000's (Godin and Fortier, 2010b, 2012b) and have stabilized since. Polygons geometry and instruments specifications are detailed in Table 1.

2.2 Instruments, data acquisition and processing

2.2.1 Air and ground temperature

Polygons were drilled in 2012 using a portable permafrost core-drill system and the boreholes (BH), approximately one meter deep, were instrumented with a string of temperature sensors in polygons EP-A, EP-B, EP-C and IP-A (Fig. 3). Temperatures were recorded between summer 2012 and summer 2014 for these four polygons at 5, 20, 50, 90 cm deep 1. A string of thermistors installed in a borehole located in a low-center polygon distant 2 km of the gully and connected to a logger (BYLOTPD, Fig. 2) recorded ground temperature between 2010 and summer 2013 at 10, 20, 30, 40, 80 cm (Allard et al., 2014). BYLOTPD was drilled and initially instrumented in 2001 and had a sensor at the surface until 2007; this long-term series was useful when missing data occurred in the time series. Thaw depth was obtained for each site by interpolating the temperature in each borehole between sensors.

Air temperature was recorded on site between 2010 and 2014 by two stations (BYLOSIL and BYLCAMP) from the SILA network (CEN, 2014).

2.2.2 Ground moisture and cover

An array of five moisture sensors (1) were deployed in each studied polygon centers during summer 2013 to monitor the near-surface moisture regime (Figs. 3a and b). Raw volumetric water content (VWC, $m^3 m^{-3}$) was calculated using TDR sensors. Calibration of the moisture data recorded by the TDR probes was necessary (Czarnomski et al., 2005) due to the high organic content of the soils at the study site. The calibration was performed by saturating an instrumented (TDR) soil sample of known mass and volume while drying at air temperature, and weighing frequently, thus building a relation between the weight of the water in the sample and the signal in the moisture sensor. The equation derived from an exponential curve obtained from the logged data ($R^2 = 0.97$, $n = 9$), was applied to all moisture readings. For the sake of data comparison between studies (Hinzman et al., 1991; Liljedahl et al., 2011), the moisture data will be presented as percent saturation. This relative metric was determined based on the exponential curve generated during calibration and applied to all volumetric water content values.

Precipitations during summer 2013 was obtained daily using a Hellmann Rain Gauge, compact version (CEN, 2014). The snow-water equivalent relation was used to account for solid precipitations.

Maximum snow depth within and nearby the gully was obtained by time-lapse photography (daily, at noon during one year) between summer 2012 and summer 2013. The camera used was a Reconyx model PC-800 Hyperfire fixed on a tripod, with graduated poles deployed in the field of view within and nearby the gully for reference.

2.2.3 Plant characterization

As a component of a larger study (Perreault, 2012; Perreault et al., 2015), each polygon was evaluated for vegetation cover using three randomly positioned 70 cm × 70 cm quadrats in

July 2009 or 2010. Vertical photographs of the quadrats were taken at approximately 1.3 m from the ground (see detailed protocols in Chen et al. (2010)). Vascular plants, bryophyte and lichen cover were evaluated as the projection on the ground with an abundance scale modified from Daubenmire (1959) on all pictures overlain with a 7 cm grid. Mean plant cover were calculated for each polygon. Details on the methods are available in Perreault (2012).

2.2.4 Active layer depth, degree-days and n factors

Air temperature has an important influence on ground temperature. Thawing degree-days (DDT) and freezing degree days (DDF) are simple indexes used to calculate heat induction and extraction in a soil. A degree day is the difference between the mean daily temperature and 0 °C (Jumikis, 1977). The sum of the daily averages is then computed for a season with negative index being DDF (freezing season) and positive index being DDT (thawing season).

Active layer depth at the end of the thawing season for a given site can be estimated using Stefan's equation modified for permafrost conditions (Brown et al., 2000; Jumikis, 1977):

$$Z = E\sqrt{\mathrm{DDT_{air}}}$$

where Z represents the active layer depth, E the edaphic factors (or physical properties of the ground and its cover) and $\mathrm{DDT_{air}}$ the sum of the average daily air temperature above 0 °C at the site (Brown et al., 2000; Shiklomanov et al., 2010; Woo et al., 2007). $\mathrm{DDT_{air}}$ is provided by the nearby SILA stations (CEN, 2014).

Ratio between the $\mathrm{DDT_{soil}}$ (sum of thawing degree day at the soil surface) and $\mathrm{DDT_{air}}$ provide the term n_t known as the thaw season n factor (Klene et al., 2001; Lunardini, 1978) as follows:

$$n_\mathrm{t} = \frac{\mathrm{DDT_{soil}}}{\mathrm{DDT_{air}}}$$

Similarly to n_t, the term n_f is used for freezing season n factor:

$$n_\mathrm{f} = \frac{\mathrm{DDF_{soil}}}{\mathrm{DDF_{air}}}$$

where DDF_{soil} and DDF_{air} respectively stand for freezing degree-day at the ground surface and freezing degree-day of air. DDF_{soil} and DDT_{soil} were provided by near-surface sensors buried at 0.05 m in polygons EP-B and IP-A (BH location in Figs. 2 and 3).

Near surface thermal gradients were calculated for sites BYLOTPD (10–20 cm), EP-B and IP-A (5–20 cm) during August 2012 for summer and January 2013 for winter. Thermal gradient can be computed as:

$$i = \frac{T_s - T_b}{x}$$

where i is the thermal gradient (°C m^{-1}), or the temperature change between two points in a medium, T_s and T_b are the temperature at the surface and bottom and x the depth (thickness) of the layer considered in the measurements (Jumikis, 1977).

2.2.5 Statistics and landscape modelling

Quantitative analyses were performed with R (R Core Team, 2014). The graphics were prepared with the ggplot2 module.

Site micro-topography was obtained using a Trimble VX station in survey mode (prism), where 92 to 210 spatially referenced points were recorded for each polygon and their proximal area (polygon center, ridge, troughs, nearby retrogressive thaw slumps or gully network branches). Surveyed points had an accuracy of ±1cm. In polygon centers, organic mat, mosses were either relatively thin (at most 5cm thick) or sparse enough to deploy the survey pole on the ground. Ridges and gully slopes were sparsely vegetated and consequently the survey pole was in direct contact with the ground. Surveyed spatial data was loaded and processed in ESRI's ArcGIS v10. An interpolation (Gaussian process regression) was applied to the points to create a 3D surface. A GeoEYE (1 pixel = 0.5m) satellite image was used as background with an infra-red, red and green false color rendering in Figure 2 (2 September 2010).

3 Results

3.1 Ground moisture and cover

3.1.1 Winter dynamics

Near the gully, a continuous snow cover overlaid the polygons (IP-A, EP-A, EP-B and EP-C) between late September until mid-May 2013, when the blanket started to be fragmented. The polygons adjacent to the gully had a snow cover of at most 10 cm deep during the whole winter 2012–2013. In the depressions (gully), accumulations could either be absent or thicker than 1 m deep, depending on the channel sections. Flat surfaces outside the gully acted as a source for snow and the gully channels as sinks where snow accumulated. Shallow snow cover exposing the ground to increased temperature variations during winter enabled more heat to be extracted from the ground and diminished the insulating role of snow, with a potential for a thinner maximum active layer depth. A slightly greater n_f was obtained at site EP-B (n_f 2012–2013 = 0.99 and n_f 2013–2014 = 0.88) compared to IP-A (n_f 2012–2013 = 0.99; n_f 2013–2014 = 0.88), indicating a thinner snow cover and greater heat extraction during winter. This result in a higher $\mathrm{DDF_{soil}}$ value for EP-B compared to IP-A for both monitored winters (Table 2).

3.1.2 Summer dynamics

Snowmelt enabled the formation of a shallow pond each year in the center of the intact polygon (IP-A, Fig. 3a). The pond presence was reflected by a ground saturation of 100 % in IP-A center until June 20 th, 2013 as indicated by the sensor #3 and greater than 90 % until June 21 st, 2013 for the other sensors (IP-A, Fig. 4).

The water levels and the area occupied by the pond fluctuated until it disappearance, between late June to early July 2013. Near surface moisture progressively diminished in response to evapotranspiration and the lowering of the water table following the propagation of the thaw front in the active layer and the consequent enlargement of the reservoir capacity. Between June 17th and July the 1st, 2013, the thaw front progression was 7 mm d^{-1}, followed by a rapid progression of 100 mm in 4 days. A few precipitation events (IP-A, Fig. 4, E1, E2, E3 and E5) restored the nearly saturated state for short periods.

Moisture for IP-A (Fig. 4) was quasi-uniform between the five TDR sensors deployed in its center at any given time. Standard deviation between each individual TDR in IP-A were at least 2.03 and at most 7.8 % saturation at each time step during summer 2013. During most rain events, moisture readings increased in the same direction and amplitude (IP-A, Fig. 4, E2, E3, E5 and E6) as clearly shown by the corresponding moisture peaks. Likewise, as the summer evolved, evapotranspiration diminished the overall ground moisture in the polygon consistently; further, moisture variation increased as the thaw front deepened.

While the moisture inside IP-A was quasi-uniform between sensors at any given time, the difference in moisture decreased significantly between the initial saturated state and the late summer drier state (Fig. 4 and Fig. 5). The last readings of the summer indicated saturation varying between 47.8 % and 63 % for a thaw depth of 0.5 m. Thus moisture was consistent across time at the scale of this specific polygon center. Median saturation levels varied between 82.5 % and 94.4 % during the measurement period, levels relatively close to the saturation levels (Fig. 5). Overall, moisture levels responded homogeneously to either input (rain) and output (evapotranspiration) at all monitored locations inside this polygon and it stayed moist during summer.

Near-surface ground moisture conditions evolved differently in eroded polygons EP-A, EP-B (Fig. 3a) and EP-C (Fig. 3b) compared to the intact polygon IP-A (Figs. 4 and 5) when considering whether the moisture balance of individual eroded polygons (intra-polygon) and between polygons (inter-polygons).

Eroded polygons EP-A, EP-B and EP-C (Fig. 4) were characterized simultaneously by a) a strong variability in moisture saturation between sensors in their respective centers (intra-polygon); and b) a variability in overall moisture saturation between each eroded polygon (inter-polygons). Among the fifteen sensors deployed in the three eroded polygons, only two sensors (EP-A-#2 and EP-C-# 5) recorded curves which were similar (but nevertheless drier) to the wet polygon IP-A. Those two emplacements inside the eroded polygons were near saturation (~ 90 % saturation) at the beginning of the logging interval

, had moisture peak recorded when precipitation events E1, E3 and E5 occurred and experienced a progressive decrease in moisture levels in response to evapotranspiration and thaw front deepening (EP-A-#2 median=74.4 %, min=63.7 % max=94.5 % and EP-C-# 5 median=76.7 %, min=62.9 %, max=91.3 %). At the opposite, EP-C-#1 (located ∼ 1 m from EP-C-#2 mentioned above) had a median moisture saturation of 33.5 %, underlining significant differences in moisture inside the same polygon (Fig. 5). For each time-step, EP-C moisture intra-polygon readings were the most variable: standard deviation for the duration of the record was at least 14.2 and at most 18.1 % saturation.

More stable ground moisture levels were also observed in eroded polygons. These moisture readings were characterized by a) a weak response to precipitation inputs, b) to evapotranspiration and thaw front deepening, when compared to the intact IP-A or single emplacement in eroded polygons (EP-A-#2 and EP-C-#5). Data recorded by all the sensors in EP-B underlined quite clearly the low variability of the readings especially as displayed by nearly linear percent saturation moisture levels (Fig. 4, EP-B) and by whisker boxes for EP-B-#2, EP-B-#5 (Fig. 5). Thaw depth was very shallow (∼ 20 cm) in some parts of the polygon EP-B (Fig. 4, EP-B, red dashed line); mean thaw depth for EP-B the July 1st, 2013 was 19 cm (SD = 4). Sensors located 1.5 m on each side of EP-B-2 (EP-B-1 and EP-B-3) provided non-overlapping ranges for moisture – underlining a great variability under short distance in this disturbed polygon. Other sensors reported similar low moisture variability in EP-A and EP-C. For instance, EP-B-#2 percent moisture median was 92.8, varying during the summer between 90.7 % and 96.3 %, thus a wet emplacement in this polygon, where an adjacent sensor (EP-B-#1, located 15 m nearby) recorded drier conditions with a median of 69.9 %.

3.2 Ground temperature and active layer thickness

Ground thermal regime monitoring obtained in an intact low-center polygon (BYLOTPD) between winter 2010 and summer 2013 provided maximum active layer depth of 56, 48.5, 52 and 40 cm for respectively 2010, 2011, 2012 and 2013 (BYLOTPD, Figs. 6, 7). During these four years, the 0 °C isoline reached a depth of 10 cm between June 22nd to June

30th. Temperatures recorded at BYLOTPD surface between 2002 and 2007 indicated an average delay of 8 days for the thaw front to lower from 0 to 10 cm. Between 2010 and 2013, the thaw front usually progressed rapidly down to 29 cm deep before slowing. Initial ground thaw progression rates varied between 1.5 $cm\,d^{-1}$ up to 8 $cm\,d^{-1}$ and then slowed to less than 0.5 $cm\,d^{-1}$ until reaching the near maximum thaw depth. While the maximum thaw depth attained varied from year to year (BYLOTPD, Fig. 6), the maximum depth $\pm$2cm persisted for 40 $\pm$ 1d. In 2012, the active layer refroze slowly at first, and then very rapidly when all the latent heat was extracted from the ground. Freeze-back of the active layer was completed during the first week of October. During the 2012-2013 winter, temperature at 66 cm depth remained below $-16\,^{\circ}C$ for 121 consecutive days (violet, BYLOTPD, in Fig. 7). The shape of the $0\,^{\circ}C$ isoline contour was akin to an ellipsoid, with a rapid thaw and freeze back respectively at the beginning and the end of the summer and a relatively stable, long-standing maximum thaw depth in between.

The intact polygon IP-A located nearby the gully shared some characteristics with BYLOTPD. In 2012, IP-A and BYLOTPD had a similar maximum thaw depth (52 cm) following a similar input of thawing degree-days, respectively 450 and 474 DDT (Fig. 6). While there was some interannual variability, dispersion was limited and alike to readings from other sites (particularly 2010 to 2012, IP-A, EP-A, EP-C). All sites responded similarly for each monitored year when considering the direction of change, implying that every site had a shallower maximum thaw depth in 2013 compared with 2012, resulting from a lower DDT that year.

At the beginning of the record (July 7th) the thaw depth was at 42 cm and reached its maximum depth 52 days later (August 29th) at 52 cm deep (0.19 $cm\,d^{-1}$ during this interval). A complete thawing season was recorded in 2013, showing a rapid initial progression of the thaw front during the first nine days 1.67 $cm\,d^{-1}$ (beginning June 10th) and then a slower rate until the maximum thaw depth was attained at 50 cm. Once the deepest point was reached, it froze back in 33 days. Overall, thaw season last 94 days for IP-A during 2013. Temperature at a depth of 63 cm was below $-16\,^{\circ}C$ for 165 continuous days during the 2012-2013 winter, and 143 days during 2013-2014 (violet, IP-A, in Fig. 7). Short peaks of warm temperatures were observed in IP-A center, exceeding 8 °C; in comparison, warm peaks were not present on BYLOTPD since there were no sensors near the surface (shallowest at 10 cm). The shape of the 0 °C isoline contour of IP-A (Fig. 7) was parabola-like in 2012 and 2013.

When comparing ground thermal regime of intact polygons against sites adjacent to the gully, maximum active layer depths were within the same range for 2012 (EP-A = 47 cm, EP-C = 44.5 cm against IP-A = 52 cm and BYLOTPD = 52 cm) (Fig. 6). Active-layer depths were similar to those sites (except BYLOTPD) in 2013, with thaw initiation varying between June 8th and June 12th. In 2013, BYLOTPD maximum thaw depth was shallower than the other sites, yet followed a similar trend than most of the other sites during this colder year. EP-A and EP-C had a parabola shape evolution of the 0 °C isoline, with rapid thaw initiation and refreezing, similarly to IP-A. There was no temporal persistence of the thaw front for IP-A: once the maximum depth was reached, it started thinning the day following the maxima (for 2012 and 2013). EP-A and EP-C ground temperature at 63 cm was below −16 °C continuously during respectively 176 and 170 days (2012-2013); during 2013-2014 winter it was 168 and 163 days (violet., EP-A and EP-C, in Fig. 7).

On the other hand, EP-B had a very shallow maximum ALD with 21 and 20.5 cm recorded for 2012 and 2013, less than half of the other monitored polygons, either intact or eroded (Fig. 6). Thaw depth progressed at a rate of approximately 1 cm d^{-1} for 9 days followed by a clear slowdown toward stabilization of the thaw progression. Maximum thaw depth persisted for 59 days in 2012 and 51 days in 2013. The shape if the 0 °C isoline was akin to a trapezoid - with the rapid initial thaw, followed by a long stable maximum depth and rapid refreezing. Surface temperature peaked at 11.4 °C during summer 2013. During 2012-2013 winter, EP-B ground temperature at 63 cm was below −16 °C continuously during respectively 169 days, and 163 for 2013-2014 (violet, EP-B, in Fig. 7).

During summer of 2013, the n factor n_t was closer to 1 for IP-A than EP-B (respectively 1.02 and 1.06). Thermal gradient was steeper during summer for EP-B than for IP-A (Table 4).

The n factor n_f computed for the sites indicated values closer to 1 during winter for EP-B compared to IP-A. A n_f of 0.99 for EP-B during 2012–2013 (Table 2) clearly suggesting a thin snow cover at this location. Thermal gradient for EP-B was very steep at shallow depths with $-26 \pm 9\,^{\circ}\mathrm{C\,m^{-1}}$ (Table 4) during winter, reflecting the absence of a substantial snow cover; considerably larger than other intact sites either at Bylot Island or at other undisturbed sites. Thermal gradient in the literature during winter in the active layer or the near surface was similar for all sites except for EP-B (Table 4).

Therefore the proximity of the gully and the consequent shallow snow cover in polygons nearby the eroded channels could impact heat extraction during winter, compared with an intact polygon (BYLOTPD) where microtopography of polygon ridges and absence of gully enabled thicker cover. Near-surface averaged maximum temperatures were generally cooler in the intact polygon (BYLOTPD, $3\,^{\circ}$C) in 2012 compared with the other polygons as shown by the reddish colours delineating the $1\,^{\circ}$C isolines in Fig. 7 (EP-A, $EP-B = 8\,^{\circ}$C, $EP-C = 5\,^{\circ}$C, $IP-A = 10\,^{\circ}$C).

The year 2012 had a warmer summer than 2013 and the winter 2012–2013 was warmer than the 2011–2012 winter (Table 3). The polygons located within a 1 km radius and those near the gully were exposed to similar $\mathrm{DDT_{air}}$. Inter-polygonal differences in the active layer dynamics (e.g. moment of maximum ALD, maximum depth of the active layer, averaged values for near-surface temperature) were due to polygon-specific surface characteristics (absence of snow cover during winter and vegetation, moisture during summer) impacting ground thermal dynamics at each respective sites.

3.3 Vegetation in intact and eroded polygons

In 2010 and 2014, the center of the intact wet polygon (IP-A) was uniformly vegetated with typical wetland vegetation with low vascular plant diversity (see wetland vegetation in Perreault et al., 2015 in this issue). Perreault (2012) measured a strong cover of living mosses (*Drepanochladus* sp. 53.3 % and *Polytricum* sp. 1.3 %) and *Carex aquatilis* (27.5 %), a sparse cover of *Dupontia fisheri* (0.5 %) and traces of *Pedicularis sudetica*, *Arctagrostis latifolia* and *Salix arctica* (Supplement 1).

The three other polygons had a higher vascular plant diversity and less uniform vegetation with a mixture of wetlands and mesic species typical of disturbed polygons

(Perreault et al., 2015, this issue). Polygon EP-A had 20 vascular plant species with the higher covers for wet habitat species with dried *Drepanochladus* sp. mosses (77.5 %), *Carex aquatilis* (6 %), *Dupontia fisheri* (3 %) *Eriophorum angustifolium* (2.5 %) and *Eriophorum scheuchzeri* (1.3 %) and traces for a number of typical mesic habitat species such as *Arctagrostis latifolia*, *Cerastium alpinum*, *Luzula confusa*, *L. arctica* and *Stellaria longipes*). Polygon EP-B had a fraction of its surface with bare-ground (2.5 %), a sign of disturbance, 42.7 % of dried mosses of wet habitat *Drepanochladus* sp. and 16 vascular plant species. Wet habitat species and mesic species shared the dominance with 21 % *Eriophorum angustifolium* and 10.8 % of arctic willow (*Salix arctica*). Lastly, polygon EP-C with 11 vascular plant species was dominated by mesic habitat mosses *Aulacomnium* sp. (41.7 %) and vascular plants *Salix arctica* (19.3 %), *Arctagrostis latifolia* (3 %) and *Salix reticulata* (2.5 %). The typical wet species were not present in this polygon anymore (Perreault et al., 2015).

4 Discussion

4.1 Terrain heterogeneity

4.1.1 Intact polygons

The comparison of shallow ground thermal regime between IP-A and BYLOTPD showed that similar terrain located only a few kilometers apart in an similar terrain can behave slightly differently in response to local conditions. For those two intact sites, the active layer depth for most years (figs. 6) was within similar ranges, but the shape of the 0 °C isoline and the timing of ground thaw initiation differed slightly 7, implying site-distinct edaphic factors. Thermal gradients was greater for IP-A than for BYLOTPD (table 4). This is interpreted as the result of differential lateral subsurface water flow between these two sites. Indeed, the presence of a gully nearby IP-A favored drainage which reduced subsurface flow whereas BYLOTPD had no such gully effect during the thaw season. Also, snow cover dynamics may differ in a similar manner between two such polygons, with an increased possibility of snow being blown from a polygon into the gully. This is reflected by colder temperatures at 60 cm depth during winter for BYLOTPD compared to the other sites (violet, in BYLOTPD fig. 7). Polygon IP-A was self contained (intact rims) which enabled intra-polygonal moisture homogeneity in its center along the monitoring transect (fig. 5). *Carex aquatilis*, dominant species in this polygon (Supplement 1), was an efficient competitor in such stable and wet environments (Billings and Peterson, 1980).

4.1.2 Eroded polygons

Neighboring (IP-A, EP-A and EP-B) and nearby (EP-C) polygons had less environmental variability among each other because of their proximity. The eroded polygons were all located very near a gully, their topographic gradient was alike and their proximity to a topographic low (gully bottom) was similar. What varied was the length of their contour adjacent to the gully, the integrity of their ridge and their intrinsic potential to retain moisture in their center, including the capacity to retain a snow during winter.

Previous to 1999 and previous to gully inception, these eroded polygons were low-center polygons (Godin and Fortier, 2012b), with similar surface conditions. When erosion initiated in 1999, not every site was affected in the same way: EP-A had a secondary ice wedge melted in the center of EP-A, creating a linear trench and reducing ground moisture at all monitoring sites. However it was observed that some parts of the center were able to maintain wet conditions even up to 14 years after degradation (EP-A-#1, #2 and #3) (fig. 4 and 5). This result stresses the heterogeneous character of moisture within eroded polygon centers. This situation translated into more micro-habitats and higher plant diversity (20 vascular species, see supplement 1) and the presence of plants typical of stable wet environments (*Carex aquatilis*) and a specie efficient in colonizing wet environments (*Dupontia fisheri*) Billings and Peterson (1980) or when water supply was uncertain (Bliss and Gold, 1994).

EP-C's moisture signature in this well-drained polygon shared characteristics with EP-A. Differential thaw-subsidence in the center changed the polygon microtopography and gave rise to some wetter and drier areas, although to a lesser extent than EP-A (5). One sensor

(EP-C-#1) in particular had a low moisture saturation through the recording interval: such an intra-polygon heterogeneity and consequent moisture conditions favored the growth of plants that were either rare or absent from IP-A (Supplement 1; *Salix arctica*, *S. reticulate* and *Arctagrostis latifolia*).

EP-B's thermal regime and the moisture signature were strikingly different from observations in the other polygons. Active layer was thin and with a persistent maximum thaw depth at the borehole emplacement during summer. A thin active layer resulted in extreme thermal gradients, very high during winter and summer (Table 4). Two sides exposed to the gully contributed to a shallow snow cover during winter, enabling heat to be further extracted from its center. Thinning of the active layer resulted into the aggradation of ground ice as the permafrost table rose up. Therefore thaw depth progression was closely connected with the sum of the DDT_{air} for intact polygons, which is uncertain with an eroded site. The thinning of the active layer further implied local ground ice, carbon and nutrient fixation due to freezing following upward permafrost aggradation, but very locally. Moisture conditions varied considerably over very short distances. Thinning of the active layer also contributed to reduce the potential volume to retain water and contributed to keep the water table close to the surface. Intra-polygonal heterogeneity in moisture conditions resulted in a plant distribution including wet and mesic species along with dead mosses and vascular plant, remnants of the previous wetter state of the polygon. These results indicate that degraded low-center polygons switch from relatively homogeneous wet conditions to heterogeneous conditions in moisture, thermal conditions and plant distribution.

When impacted with erosion, polygons centers physical characteristics do not necessarily tend to all change toward the same trend. Three nearby eroded polygons in the same gully network, eroded at approximately the same time, shared a diminution (more of less severe) of the ground moisture, and not in a uniform way inside each respective polygon. Thermal dynamics during summer were more complex than those of winter; individual sites albedo, nature of the cover, moisture and ground temperature need to be taken into consideration to precisely identify differences between sites.

4.2 The question of scale: time and space

The polygon terraces characterizing the floor of the valley of glacier C-79 is the product of thousand of years of eolian sedimentation, organic and ground ice sedimentation along with syngenetic growth of ice wedges and cracking under cold conditions. Development of ridges created low-center polygons and under certain terrain conditions, groups of polygons evolved into high-center polygons as their ridges were gradually eroded.

In low-center polygon terraces, when the proper conditions are met, large gullies may form very rapidly (Fortier et al., 2007) with yearly rates of ice-wedge erosion greater than several 10's of meters per years. The erosional processes will be very dynamic and occurs rapidly immediately following the triggering events as the components of the landscape in disequilibrium are in transition and unstable (**?**). Gully channels ranged in dimensions as small as $1-2$ m wide and deep and smaller trenches were observed to further connect polygons to the gully (fig. 3), to large channels measuring more than 10 m wide and 4 m deep, networked in kilometer long channels Godin et al. (2014), thus fragmenting the terrace. Once initiated, not only it could take years (and decades) for erosion to stabilize (Godin and Fortier, 2012a), but the gully may capture and facilitate the water fluxes downstream, enabling enhanced drainage and soil displacement outside the watershed (Fortier et al., 2015; Godin et al., 2014). At medium spatial scale, more than a thousand polygons were directly eroded following gullying in this valley, with various levels of severity. As a result some polygons were completely eroded (baydzherakhii), other severely reduced in area as two sides of or more were eroded. At the fine spatial scale, polygon perturbed such as EP-A and EP-B which have a ridge or two eroded and most of their internal area intact experienced physical surface changes as well.

As the gully evolve over the years, the drainage network found alternative paths downstream. Water entry points were abandoned as the gully evolved upstream and retrogressive thaw slumps were stabilizing near an axis end when a stream was not accelerating the erosion process (Godin and Fortier, 2012b). The capacity of eroded polygon to retain water and moisture stayed diminished compared to intact polygons through time, even though they are in the course of stabilization toward their new equilibrium state. Polygons in the current study were in transition toward the new equilibrium – changes in surface conditions caused non-linear fluctuations in the active layer depth, moisture content and plant species distribution and occurrence. In any cases, the eroded polygons definitely will not return to their pre-erosion state. The gully network across the polygons constitutes a fragmentation of an otherwise flat terrain unit with an improved drainage network and drier polygons in a wider area than only the one directly linked to the gully, potentially diminishing the flux of the lateral flow. Instead of a flat, continuous terrace, gullies fragment the terrace and affect stream circulation and water recharge potential. The terrace should be a drier overall place than before gullies formed, with a more heterogeneous environment (and wet simultaneously), this being the new steady state.

Medium scale studies monitoring gully channels and other erosion morphologies, do not provide quantitative information on how polygons adjacent to the gully could be affected. Terrain heterogeneity following permafrost erosion and how the hydrologic system evolves thereafter is essential when modeling methane and carbon emissions: a model by Cresto-Alein et al. (2013) took into account the local heterogeneity of polygonal terrain and satisfactorily compared against GHG emissions measured on the field. Eroded polygons by gullying as presented in this paper underlined how a study at fine scale could result in identifying different impacts of adjacent sites eroded in a similar manner. Fine scale changes such as variable moisture in a single polygon, changing ground thermal regime and consequent heterogeneity of plant cover in an eroded polygon are major impacts as thousands of polygons are subject to erosion. When the gully and the eroded polygons stabilize and a new equilibrium state is attain, heterogeneous conditions characterize those stabilized surfaces compared to the more uniform intact polygons.

4.3 Limitations

Once triggered, as already demonstrated in previous papers (Godin and Fortier, 2012b; Fortier et al., 2007), a gully can change quite fast by very rapidly impact nearby polygons. Yet, gully inception (triggering) observation in the field were exceptional: once in 1999 -

others were observed but were not instrumented. Historical air imagery was quite useful to assess the period of initiation and evolution of several large gullies (Godin and Fortier, 2012a). However, precise or finer scale observations of active layer depth, ground temperature and ground moisture were only obtained during the last few years.

5 Conclusions

In the valley of the Glacier C-79 on Bylot Island, the rapid thermo-erosion of permafrost leading to gullies enabled the disturbance of ice-wedge polygons and consequently causing mass transfers such as water, sediment, peat transport, permafrost and massive ice thaw. The gully changed fluxes of heat and matter in the geosystem; once the gully stabilized it exists as a new steady state permanently distinct from the initial conditions. Polygons adjacent to the gully can be partially impacted at various degrees of severity. Gully effects on polygons can be partial erosion and subsidence of the ground inducing differential microtopography, ground moisture retention capacity (rain and snow), thermal conditions (via water and snow) and thus active layer thickness. Such changes in a polygon have impacts on ground ice conditions, the carbon and nutrients cycle. These differential conditions create heterogeneity at a fine scale in eroded polygons, where colder, warmer, wet and mesic conditions can co-exist in the proximity of the same polygon center and adjacent polygons. These differential conditions affects plants distribution, diversity and abundance. Vegetation will have an effect on physical, biogeochemical properties of the active layer dynamics on the long term, but more research and monitoring is needed to understand these trajectories.

The Supplement related to this article is available online at doi:10.5194/bgd-0-1-2015-supplement.

Acknowledgements. Comments by Anonymous Referees #1 and #2 were very enlightening and their suggestions useful, we are grateful for their input. We are very thankful to Gilles Gauthier and his team (Center for Northern Studies) for welcoming us to his research station and providing access to field logistics. Our project was made possible due to the financial/field support by the following organizations: Parks Canada Staff (Sirmilik), the Polar Continental Shelf Program, the Northern Scientific Training Program by the Canadian Polar Commission, ArcticNet, the ArcticWOLVES IPY program, NSERC, NSERC-ADAPT, NSERC-Discovery, FRQNT, the W. Garfield Weston Foundation and the Département de Géographie de l'Université de Montréal.

We are extremely grateful to Naïm Perreault, Stéphanie Coulombe, Laurent Lamarque, Michel Paquette, Audrey Veillette, Dr. Michel Allard, Sabine Veuille, Gabrielle Létourneau, Laurent Gosselin and Josée Turcotte for their help in the field, discussions on methods, concepts and preparation of the manuscript.

References

Allard, M. and Kasper, J. N.: Temperature conditions for ice wedge cracking: field measurements from Salluit, northern Québec, in: Proceedings of the Seventh International Conference on Permafrost, Yellowknife, Canada, Collection Nordicana, Centre d'études nordiques, Université Laval, Québec, 23––27 June 1998, Yellowknife, NWT, Canada, 5–12, 1998.

Allard, M., Sarrazin, D., and L'Hérault, E.: Borehole monitoring temperatures in northeastern Canada, v. 1.2 (1988–2014), Nordicana D8, doi:10.5885/45291SL-34F28A9491014AFD, 2014.

Ballantyne, C. K.: Periglacial Landforms | Patterned Ground, Elsevier, Oxford, 2182–2191, doi:10.1016/B0-44-452747-8/00107-1, 2007.

Billings, W. D. and Peterson, K. M.: Vegetational change and ice-wedge polygons through the thaw-lake cycle in Arctic Alaska, Arctic Alpine Res., 12, 413–432, doi:10.2307/1550492, 1980.

Black, R. F.: Periglacial features indicative of permafrost: ice and soil wedges, Quaternary Res., 6, 3–26, doi:10.1016/0033-5894(76)90037-5, 1976.

Bliss, L. C. and Gold, W. G.: The patterning of plant communities and edaphic factors along a high arctic coastline: implications for succession, Canadian Journal of Botany, 72, 1095–1107, doi:10.1139/b94-134, 1994.

Bouchard, F., Laurion, I., Preskienis, V., Fortier, D.,Xu, X. and Whiticar, M.: Modern to millennium-old greenhouse gases emitted from ponds and lakes of the Eastern Canadian Arctic (Bylot Island, Nunavut), Biogeosciences, 12, 7279-7298, doi:110.5194/bg-12-7279-2015, 2015.

Boudreau, L. D. and Rouse, W. R.: The role of individual terrain units in the water balance of wetland tundra, Clim. Res., 5, 31–47, 1995.
Brown, J., Hinkel, K. M., and Nelson, F. E.: The circumpolar active layer monitoring (CALM) program: research designs and initial results 1, Polar Geography, 24, 166–258, doi:10.1080/10889370009377698, 2000.
CEN: Environmental data from Bylot Island in Nunavut, Canada, v. 1.4 (1992–2014), Nordicana D2, doi:10.5885/45039SL-EE76C1BDAADC4890, 2014.
Chen, Z., Chen, W., Leblanc, S. G. and Henry, G. H.: Digital photograph analysis for measuring percent plant cover in the Arctic, Arctic, 63, 315–326, 2010.
Cresto Aleina, F., Brovkin, V., Muster, S., Boike, J., Kutzbach, L., Sachs, T. and Zuyev, S.: A stochastic model for the polygonal tundra based on Poisson–Voronoi diagrams, Earth System Dynamics, 4, 187–198, doi:10.5194/esd-4-187-2013, 2013.
Czarnomski, N. M., Moore, G. W., Pypker, T. G., Licata, J., and Bond, B. J.: Precision and accuracy of three alternative instruments for measuring soil water content in two forest soils of the Pacific Northwest, Can. J. Forest Res., 35, 1867–1876, doi:10.1139/x05-121, 2005.
Daubenmire, R.: A canopy-coverage method of vegetational analysis, Northwest Sci., 33, 43–64, 1959.
Dostovalov, B. N. and Popov, A. I.: Polygonal systems of ice-wedges and conditions of their development, in: Proceedings of the First International Conference on Permafrost, vol. 1, National Academy of Sciences-National Research Council, 11–15 November 1963, Lafayette, Indiana, USA, 102–105, 1963.
Environment Canada: Canadian Climate Normals, 1981–2010, Pond Inlet, available at: http://climate.weather.gc.ca/climate_normals/ (last access: 24 July 2015), 2014.
Fortier, D. and Allard, M.: Late Holocene syngenetic ice-wedge polygons development, Bylot Island, Canadian Arctic Archipelago, Can. J. Earth Sci., 41, 997–1012, doi:10.1139/e04-031, 2004.
Fortier, D. and Allard, M.: Frost-cracking conditions, Bylot Island, Eastern Canadian Arctic Archipelago, Permafrost Periglac., 16, 145–161, doi:10.1002/ppp.504, 2005.
Fortier, D., Allard, M., and Shur, Y.: Observation of rapid drainage system development by thermal erosion of ice wedges on Bylot island, Canadian Arctic Archipelago, Permafrost Periglac., 18, 229–243, 2007.
Fortier, D., Godin, E., Lévesque, E., Veillette, A. and Lamarque, L. : Thermal erosion of ice-wedge polygon terrains changes fluxes of energy and matter of permafrost geosystems, Abstract GC22C-04 presented at 2015 Fall Meeting, AGU, San Francisco, Calif., 14–18 December, 2015.

French, H. M.: The Periglacial Environment, 3rd edn., John Wiley and Sons, Chichester, England, Hoboken, NJ, 2007.

Gangodagamage, C., Rowland, J. C., Hubbard, S. S., Brumby, S. P., Liljedahl, A. K., Wainwright, H., Wilson, C. J., Altmann, G. L., Dafflon, B., Peterson, J., Ulrich, C., Tweedie, C. E., and Wullschleger, S. D.: Extrapolating active layer thickness measurements across Arctic polygonal terrain using LiDAR and NDVI data sets, Water Resour. Res., 50, 6339–6357, doi:10.1002/2013WR014283, 2014.

Gauthier, G., Rochefort, L., and Reed, A.: The exploitation of wetland ecosystems by herbivores on Bylot island, Geosci. Can., 23, 253–259, 1996.

Gauthier, G., Giroux, J.-F., Reed, A., Béchet, A., and Bélanger, L.: Interactions between land use, habitat use, and population increase in greater snow geese: what are the consequences for natural wetlands?, Glob. Change Biol., 11, 856–868, doi:10.1111/j.1365-2486.2005.00944.x, 2005.

Gauthier, G., Berteaux, D., Bety, J., Tarroux, A., Therrien, J. F., McKinnon, L., Legagneux, P., and Cadieux, M. C.: The tundra food web of Bylot Island in a changing climate and the role of exchanges between ecosystems, Ecoscience, 18, 223–235, 2011.

Gauthier, G., Béty, J., Cadieux, M.-C., Legagneux, P., Doiron, M., Chevallier, C., Lai, S., Tarroux, A., and Berteaux, D.: Long-term monitoring at multiple trophic levels suggests heterogeneity in responses to climate change in the Canadian Arctic tundra, Philos. T. R. Soc. B, 368, 20120482, doi:10.1098/rstb.2012.0482, 2013.

Godin, E. and Fortier, D.: Geomorphology of thermo-erosion gullies – case study from Bylot Island, Nunavut, Canada, in: Proceedings of the Sixty-Third Canadian Geotechnical Conference & Sixth Canadian Permafrost Conference, vol. 1, Calgary, Canada, 1540–1547, 12–16 15 September 2010, Calgary, Alberta, Canada, available at: http://pubs.aina.ucalgary.ca/cpc/CPC6-1540.pdf, 2010b.

Godin, E., and Fortier, D.: Fine-scale spatio-temporal monitoring of multiple thermo-erosion gully development on Bylot Island, Eastern Canadian Archipelago, in: Proceedings of the Tenth International Conference on Permafrost, vol. 1, edited by: Hinkel, K. M., The Northern Publisher Salekhard, 125–130, 25–29 June 2012, Salekhard, Russia, available at: http://ipa.arcticportal.org/meetings/international-conferences, (last access: 24 July 2015), 2012a.

Godin, E. and Fortier, D.: Geomorphology of a thermo-erosion gully, Bylot Island, Nunavut, Canada, Can. J. Earth Sci., 49, 979–986, doi:10.1139/e2012-015, 2012b.

Godin, E., Fortier, D., and Coulombe, S.: Effects of thermo-erosion gullying on hydrologic flow networks, discharge and soil loss, Environ. Res. Lett., 9, 105010, doi:10.1088/1748-9326/9/10/105010, 2014.

Helbig, M., Boike, J., Langer, M., Schreiber, P., Runkle, B. K., and Kutzbach, L.: Spatial and seasonal variability of polygonal tundra water balance: Lena River Delta, northern Siberia (Russia), Hydrogeol. J., 21, 133–147, doi:10.1007/s10040-012-0933-4, 2013.

Hinzman, L. D., Kane, D. L., Gieck, R. E., and Everett, K. R.: Hydrologic and thermal properties of the active layer in the Alaskan Arctic, Cold Reg. Sci. Technol., 19, 95–110, doi:10.1016/0165-232X(91)90001-W, 1991.

Inland Water Branch: Bylot Island Glacier Inventory: Area 46201, Department of Energy, Mines and Resources, Ottawa, 76 pp., 1969.

Jia, G. J., Epstein, H. E., and Walker, D. A.: Greening of arctic Alaska, 1981–2001, Geophys. Res. Lett., 30, 2067, doi:10.1029/2003GL018268, 2003.

Jorgenson, M. T. and Osterkamp, T. E.: Response of boreal ecosystems to varying modes of permafrost degradation, Can. J. Forest Res., 35, 2100–2111, doi:10.1139/x05-153, 2005.

Jorgenson, M. T., Shur, Y. L. and Pullman, E. R.: Abrupt increase in permafrost degradation in Arctic Alaska, Geophys. Res. Lett., 33, L02503, doi:10.1029/2005GL024960,2006.

Jumikis, A. R.: Thermal Geotechnics, Rutgers University Press, New Brunswick, N. J., 1977.

Klene, A. E., Nelson, F. E., Shiklomanov, N. I., and Hinkel, K. M.: The n-factor in natural landscaper: variability of air and soil-surface temperatures, Kuparuk River basin, Alaska, USA, Arct. Antarct. Alp. Res., 33, 140–148, doi:10.2307/1552214, 2001.

Liljedahl, A. K., Hinzman, L. D., Harazono, Y., Zona, D., Tweedie, C. E., Hollister, R. D., Engstrom, R. and Oechel, W. C.: Nonlinear controls on evapotranspiration in arctic coastal wetlands, Biogeosciences, 8, 3375–3389, doi:10.5194/bg-8-3375-2011, 2011.

Liljedahl, A. K., Hinzman, L. and Schulla J.: Ice-Wedge polygon type controls low-gradient watershed-scale hydrology, in: Proceedings of the Tenth International Conference on Permafrost, vol. 1, edited by: Hinkel, K. M., The Northern Publisher Salekhard, 231–236, 25–29 June 2012, Salekhard, Russia, available at: http://ipa.arcticportal.org/meetings/international-conferences, (last access: 4 December 2015), 2012.

Lunardini, V. J.: Theory of n-factors and correlation of data, in: Proceedings of the Third International Conference on Permafrost, 10—13 July 1978, Edmonton, Alberta, Canada, vol. 1, 40–46, 1978.

Mackay, J. and MacKay, D.: Snow cover and ground temperatures, Garry Island, N. W. T, Arctic, 27, 287–296, 1974.

Mackay, J. R.: The first 7 years (1978–1985) of ice wedge growth, Illisarvik experimental drained lake site, western Arctic coast, Can. J. Earth Sci., 23, 1782–1795, doi:10.1139/e86-164, 1986.
Massé, H., Rochefort, L., and Gauthier, G.: Carrying capacity of wetland habitats used by breeding greater snow geese, The Journal of Wildlife Management, 65, 271–281, doi:10.2307/3802906, 2001.
Minke, M., Donner, N., Karpov, N., de Klerk, P., and Joosten, H.: Patterns in vegetation composition, surface height and thaw depth in polygon mires in the Yakutian Arctic (NE Siberia): a microtopographical characterisation of the active layer, Permafrost Periglac., 20, 357–368, doi:10.1002/ppp.663, 2009.
Myers-Smith, I. H., Forbes, B. C., Wilmking, M., Hallinger, M., Lantz, T., Blok, D., Tape, K. D., Macias-Fauria, M., Sass-Klaassen, U., Lévesque, E., Boudreau, S., Ropars, P., Hermanutz, L., Trant, A., Collier, L. S., Weijers, S., Rozema, J., Rayback, S. A., Schmidt, N. M., Schaepman-Strub, G., Wipf, S., Rixen, C., Ménard, C. B., Venn, S., Goetz, S., Andreu-Hayles, L., Elmendorf, S., Ravolainen, V., Welker, J., Grogan, P., Epstein, H. E., and Hik, D. S.: Shrub expansion in tundra ecosystems: dynamics, impacts and research priorities, Environ. Res. Lett., 6, 045509, doi:10.1088/1748-9326/6/4/045509, 2011.
Perreault, N.: Impact of permafrost gullying on wetland habitat, Bylot Island, Nunavut, Canada, M.S. thesis, Thesis, UQTR, Trois-Rivières, Québec, Canada, 2012.
Perreault, N., Levesque, E., Fortier, D., and Lamarque, L. J.: Thermo-erosion gullies boost the transition from wet to mesic vegetation, Biogeosciences Disc., 2015.
R Core Team: R: a Language and Environment for Statistical Computing, R Foundation for Statistical Computing, Vienna, Austria, available at: http://www.R-project.org/ (last access: 24 July 2015), 2014.
Shiklomanov, N. I., Streletskiy, D. A., Nelson, F. E., Hollister, R. D., Romanovsky, V. E., Tweedie, C. E., Bockheim, J. G., and Brown, J.: Decadal variations of active-layer thickness in moisture-controlled landscapes, Barrow, Alaska, J. Geophys. Res.-Biogeo., 115, G00I04, doi:10.1029/2009JG001248, 2010.
Tranvik, L. J., Downing, J. A., Cotner, J. B., Loiselle, S. A., Striegl, R. G., Ballatore, T. J., Dillon, P., Finlay, K., Fortino, K., Knoll, L. B., Kortelainen, P. L., Kutser, T., Larsen, S., Laurion, I., Leech, D. M., McCallister, S. L., McKnight, D. M., Melack, J. M., Overholt, E., Porter, J. A., Prairie, Y., Renwick, W. H., Roland, F., Sherman, B. S., Schindler, D. W., Sobek, S., Tremblay, A., Vanni, M. J., Verschoor, A. M., von Wachenfeldt, E., and Weyhenmeyer, G. A.: Lakes

and reservoirs as regulators of carbon cycling and climate, Limnol. Oceanogr., 54, 2298–2314, doi:10.4319/lo.2009.54.6_part_2.2298, 2009.

Walker, D. A., Epstein, H. E., Gould, W. A., Kelley, A. M., Kade, A. N., Knudson, J. A., Krantz, W. B., Michaelson, G., Peterson, R. A., Ping, C. L., Raynolds, M. K., Romanovsky, V. E. and Shur, Y.: Frost-boil ecosystems: complex interactions between landforms, soils, vegetation and climate, Permafrost Periglac., 15, 171–188, doi:10.1002/ppp.487, 2004.

Watanabe, T., Matsuoka, N., and Christiansen, H. H.: Ice- and soil-wedge dynamics in the Kapp Linné Area, Svalbard, investigated by two- and three-dimensional GPR and ground thermal and acceleration regimes, Permafrost Periglac., 24, 39–55, doi:10.1002/ppp.1767, 2013.

Woo, M. K. and Young, K.: Wetlands of the Canadian Arctic, book section 229, in: Encyclopedia of Earth Sciences Series, Springer Netherlands, 902–914, doi:10.1007/978-1-4020-4410-6_229, 2012.

Woo, M.-K., Mollinga, M., and Smith, S. L.: Climate warming and active layer thaw in the boreal and tundra environments of the Mackenzie Valley, Can. J. Earth Sci., 44, 733–743, doi:10.1139/e06-121, 2007.

Zoltai, S. C. and Tarnocai, C.: Perennially Frozen peatlands in the Western Arctic and subarctic of Canada, Can. J. Earth Sci., 12, 28–43, doi:10.1139/e75-004, 1975.

Table 1. Sites specifications, presenting polygons ID, state (either intact or eroded) size (major and minor axis) and sensors deployed. A complete gully erosion map model was presented in (Godin and Fortier (2012b), Figure 3). Size was obtained by measuring the length and the width of each polygon by calculating the distance from the highest point of surrounding ridges, near their troughs. The Campbell Scientific temperature sensors (107-L) and Omega Type-T thermocouples were connected to a CR1000 datalogger. The Onset S-TMB-M006 temperature sensor was linked to a H21-002 Microstation. Moisture data acquisition systems from Decagon consisted in four to five TDR sensors (EC-5) per polygon connected to a Em5b logger. BYLOTPD is instrumented with a 3 m long custom-made thermistor cable (CEN, 2014). Temperature sensors were installed in boreholes identified as BH in Figures 3a and 3b.

ID	State	Size (m)	Depth (cm)	Temperature sensors	Moisture sensor
EP-A	Eroded	20 ×12	5	Onset UTBI-001	Decagon EC-5
			20	Campbell Sci. 107-L	
			50, 92	Omega Type-T	
EP-B	Eroded	11 ×11	5	Onset UTBI-001	Decagon EC-5
			20	Campbell Sci. 107-L	
			50, 82	Omega Type-T	
EP-C	Eroded	20 ×20	5, 25, 50, 95	Onset S-TMB-M06	Decagon EC-5
IP-A	Intact	11 ×11	5	Onset UTBI-001	Decagon EC-5
			20	Campbell Sci. 107-L	
			50, 90	Omega Type-T	
BYLOTPD	Intact	12 ×12	10, 20, 30, 40, 80	Custom thermistors	N/A

Table 2. Degree-days of freezing (DDF_{air}) as recorded by the on-site meteorological stations, between 2010 and 2014 (CEN, 2014), and DDF_{soil} for EP-B and IP-A (winter 2012–2013 and 2013–2014). The length of the thawing season is indicated for each measured unit under their respective n day column.

Winter	n day	DDF_{air}	n day	DDF_{soil} IP-A	n day	DDF_{soil} EP-B
2010–2011	256	5331				
2011–2012	262	5343				
2012–2013	271	4922	260	4698	260	4846
2013–2014	272	5674	265	4834	256	5015

Table 3. Degree-days of thawing (DDT_{air}) as recorded by the on-site meteorological stations, between 2010 and 2014 (CEN, 2014), and DDT_{soil} for EP-B and IP-A (summer 2013). The length of the thawing season is indicated for each measured unit under their respective n day column.

Summer	n day	DDT_{air}	n day	DDT_{soil} IP-A	n day	DDT_{soil} EP-B
2010	114	526				
2011	97	556				
2012	96	495				
2013	98	450	92	459	93	476

Table 4. Thermal gradients reported from the literature (as reference) and from sites in this study (EP-B, IP-A). The gradient i °C m^{-1}, the depth, the season, the location and the source are mentioned. Winter thermal gradient were common while spring/summer gradients sparser.

i, °C m^{-1}	Depth (m)	Season	Location	Source
2.5 to 11	0–0.5	Spring	Bylot Isl., NU, CA	Fortier and Allard (2005)
$-10.9 \pm (-3.9 - 18.9]$	0–0.4	Winter	Bylot Isl., NU, CA	Fortier and Allard (2005)
-15 to -10	0–0.45	Winter	Illisarvik LK, NWT, CA	Mackay (1986)
10	Near surf.	Winter	Salluit, QC, CA	Allard and Kasper (1998)
Less than -15	0–0.25	Winter	Svalbard, NO	Watanabe et al. (2013)
-15 to -7	0.25–0.75	Winter	Svalbard, NO	Watanabe et al. (2013)
0.5 to 5	0–0.4	Summer	Brooks Range, AK, USA	Hinzman et al. (1991)
-8 to -1	0–0.4	Winter	Brooks Range, AK, USA	Hinzman et al. (1991)
$2 \pm 1(1\sigma)$	0.1–0.2	Summer	Bylot Isl., NU, CA	BYLOTPD (this study)
$-13 \pm 3(1\sigma)$	0.1–0.2	Winter	Bylot Isl., NU, CA	BYLOTPD (this study)
$-26 \pm 9(1\sigma)$	0.05–0.2	Winter	Bylot Isl., NU, CA	EP-B (this study)
$39 \pm 10(1\sigma)$	0.05–0.2	Summer	Bylot Isl., NU, CA	EP-B (this study)
$-8 \pm 3(1\sigma)$	0.05–0.2	Winter	Bylot Isl., NU, CA	IP-A (this study)
$19 \pm 6(1\sigma)$	0.05–0.2	Summer	Bylot Isl., NU, CA	IP-A (this study)

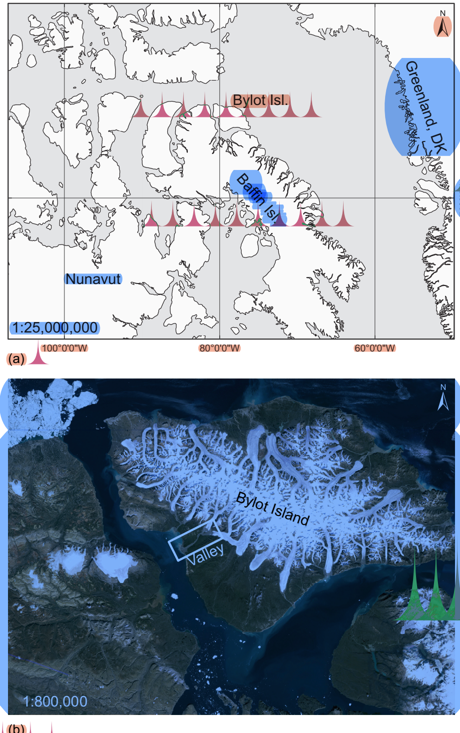

Figure 1. The study site is on Bylot Island in the Canadian Arctic archipelago (73°09′ N 79°57′ W), north of Baffin Island **(a)**. The valley of Qalikturvik is located in the south-western section of the island **(b)** (background: NRCan Landsat-7 orthorectified mosaic, 03 August 2010).

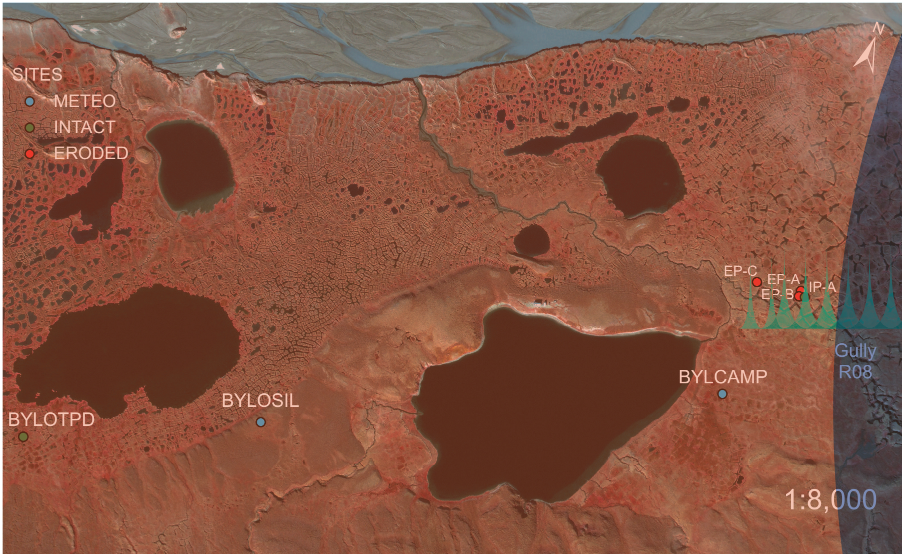

Figure 2. The location of the stations at study site; map background is a GEO-Eye false colour satellite image (Near Infra-Red, Red, Green) obtained the September 2nd 2010. BYLOSIL and BYLCAMP are meteorological stations part of the SILA network (CEN, 2014). BYLOTPD is a reference ground temperature monitoring site installed in a low-center polygon (Allard et al., 2014). The gully R08 is located on the right side of the image, N-E of the lake. Stations EP-A, EP-B, EP-C and IP-A are located near the gully margin.

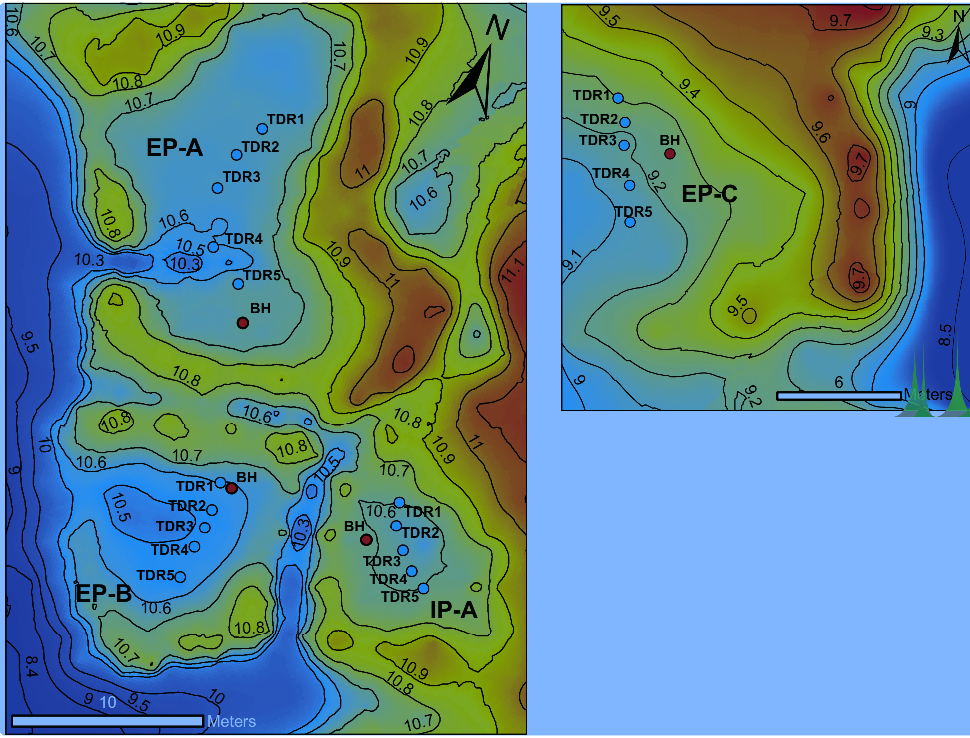

Figure 3. Digital elevation model of sites EP-A, EP-B and IP-A. Altitudinal isolines contours were digitized on the figure at each 0.1 m. A gully channel (deep blue) initiated in 1999 near polygons; rims (yellow and orange) delineates polygon contours; light blue indicates a breach by erosion in EP-A and EP-B. IP-A ridge contouring the polygon is intact. The gully channel floor (dark blue) is approximately 2 m lower than nearby polygons rims at this position. Boreholes equipped with a string of thermistors (BH in the figure) are identified in red in each polygons, and moisture sensors in blue (TDR in the figure).

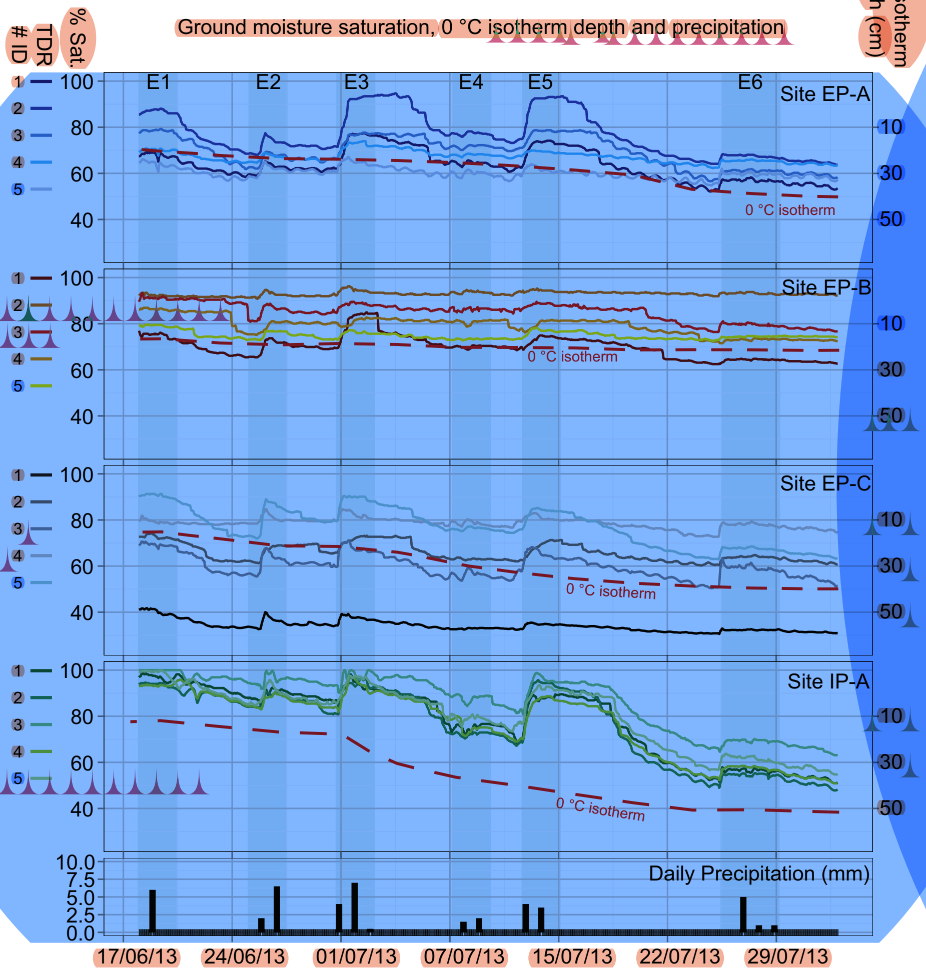
Ground moisture saturation, 0 °C isotherm depth and precipitation
TDR # ID
% Sat.
0 °C isotherm depth (cm)
E1
E2
E3
E4
E5
E6
Site EP-A
Site EP-B
Site EP-C
Site IP-A
0 °C isotherm
Daily Precipitation (mm)
17/06/13
24/06/13
01/07/13
07/07/13
15/07/13
22/07/13
29/07/13

Figure 4. Moisture readings for the near surface of sites EP-A, EP-B, EP-C and IP-A during summer 2013 (Fig. 3). Daily precipitation readings indicated 6 rain events through the summer, identified in the figure E1 to E6. Propagation of the thaw-front in the active layer evolution is identified as the 0 °C isoline for each sites – moisture levels in percent saturation decreased following active-layer depth for all sites except EP-B.

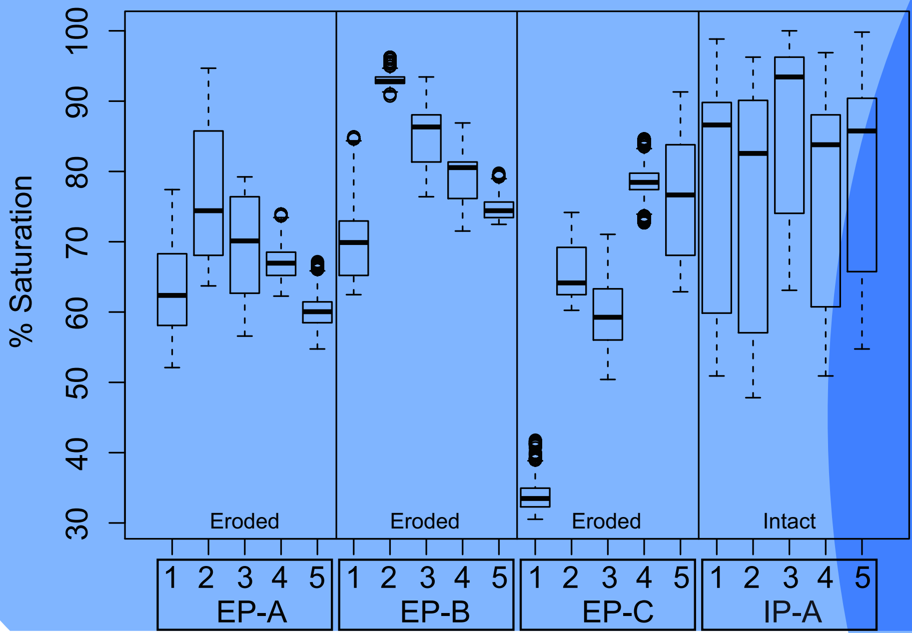

Figure 5. Variability of moisture conditions during summer 2013 (percent saturation), per polygon, for each sensor. The line located in the center of each box indicates the median, lower box line indicates the first quartile and the higher line the third quartile; points are outliers. Underlying data refers to the variability of fig. 4.

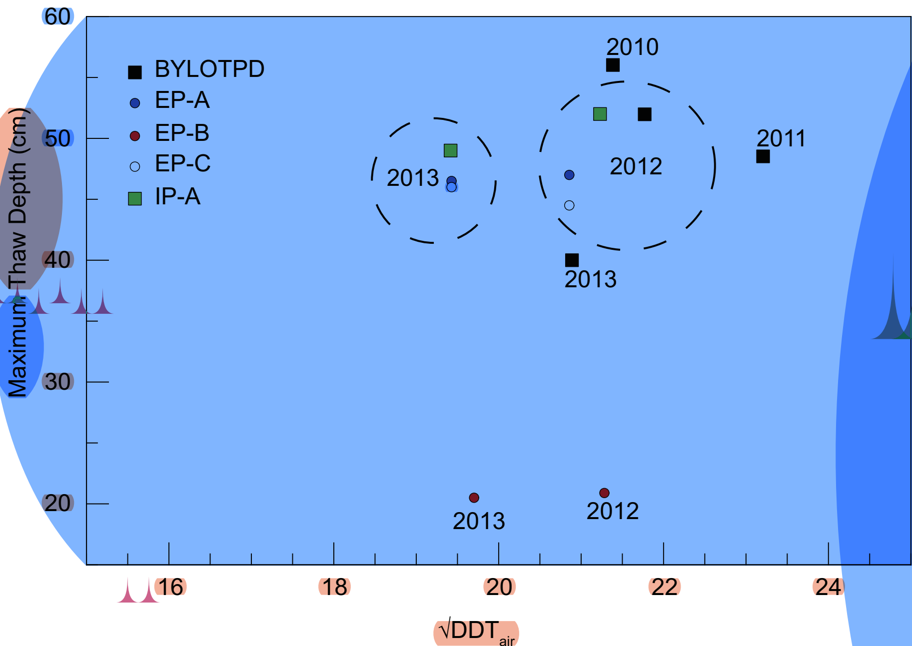

Figure 6. Maximum thaw-depth (y-axis, cm) related to the square root sum of the degree-days of thawing (x-axis, $\sqrt{DDT_{air}}$) for sites between 2010 and 2013. The relation between those two variables for the sites was similar for all locations except EP-B. Sites measured in 2012 were exposed to more DDT than in 2013, but this tendency was not reflected clearly in the maximum active-layer depth – possibly implying varying edaphic factors between both years. EP-B's depth was virtually the same between 2012 and 2013.

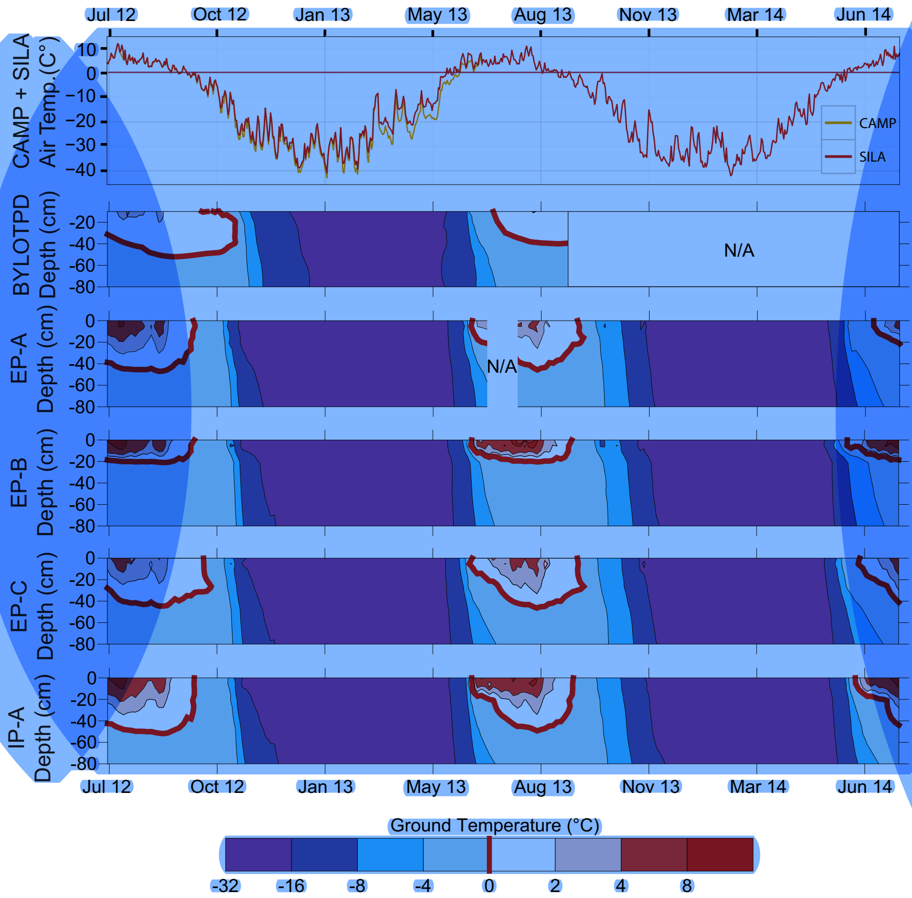
Jul 12
Oct 12
Jan 13
May 13
Aug 13
Nov 13
Mar 14
Jun 14
CAMP + SILA
Air Temp.(C°)
10
0
−10
−20
−30
−40
CAMP
SILA
BYLOTPD
Depth (cm)
EP-A
Depth (cm)
EP-B
Depth (cm)
EP-C
Depth (cm)
IP-A
Depth (cm)
0
-20
-40
-60
-80
N/A
Ground Temperature (°C)
-32
-16
-8
-4
0
2
4
8

Figure 7. Air Temp (top) represents the mean daily air temperatures from BYLCAMP (yellow) and BYLOSIL (red) recorded between July 2012 to July 2014. The 0 °C limit is highlighted in red as a reference for mean daily air temperature. BYLOTPD, EP-A, EP-B, EP-C and IP-A's top 80 cm ground thermal regime follows – purple color indicating colder temperature, reddish warmer temperature. The 0 °C isotherm of the ground temperature is indicated as a red line.